A Study of Curved Flexures for MEMS

Minhee Jun[1], and Jason V. Clark[2]
Departments of Electrical and Computer Engineering, Purdue University
West Lafayette, IN, 47906
[1]minhee.jun@gmail.com, [2]jvclark@ecn.purdue.edu

Abstract: Large deflection actuators are becoming increasingly important for microsystems. Since actuation forces are usually small, large deflection actuators usually require flexures with low stiffness. Rectangular serpentine flexures are often used for such actuators due to their low stiffness and large linear deflection range. However, the corners of rectangular serpentine flexures are subject to large stresses which may shorten their use and the corners are subject to fillets due to limitations in the fabrication process. In this paper we investigate the performance of curved serpentine flexures to the performance of rectangular serpentine flexures. We compare stress, strength, linearity range, geometric process variations, quality factor, electrical conductivity, and thermal conductivity. We find that the curved serpentine flexure has significant benefits over the conventional rectangular serpentine flexure with respect to stress, quality factor, linearity, etc.

1. Introduction

The problem of sizeable deflection actuators in microsystems has recently been given considerable attention. Of special interest in a design of actuators is to find flexures with less hardness. This is because of the limitations on supplied forces or space usage scales in microsystems. Nevertheless, the present research question emerged from a problem with large stresses on the corners of a rectangular serpentine flexure (RSF). The stresses on the corner would trigger flexure damage after a period of time. Curiously, despite the increase in studies on RSF, few researchers have attempted to address curved serpentine flexure (CSF). The major purpose in study is to take a closer look at the properties of RSF comb and the properties of CSF. We will test geometric process variations, linearity range, stress, strength, quality factor, electrical conductivity, and thermal conductivity in COMSOL simulation with the expectation of excellent performance of CSF. Geometric process variations can measure flexibility of flexures and reflect how much flexures are stretched for given voltages. The quality of displacement of geometric process variations is enumerated by linear range. Linearity guarantees easiness of manipulating displacement by supplying voltages. Finding the linear range is related to the accuracy of system control. Stresses on the comb drives are inevitable and are influenced proportionally by geometric process variations. So, a scientific hope in a stress test is stresses with fewer increments according to a given displacement increment. Strength is an electrical field induced by the electrical potential difference. The quality factor (Q factor) is a measure of the ratio between stored energy and energy lost in a free oscillation (Ref. 3). Higher Q implies the oscillations vanish more slowly because energy loss relative to the stored energy is low. Electrical conductivity is a measure of a material's ability to conduct an electric current, and thermal conductivity is a measure of a material's ability to conduct heat. Higher electrical conductivity and higher thermal conductivity represent good properties of metals.

2. Use of COMSOL Multiphysics

We will use three different types of schematics for testing characteristics of comb drives with RSF and with CSF. Each schematic is optimized appropriately for assessing comb-drive performance. Schematic A is designed for evaluations of geometric process variations, linearity range, stress, and strength. [2] Schematic B is for the evaluation of quality factor [3] while Schematic C is for the estimation of electrical conductivity and thermal conductivity [5].

Because displacement proportionally corresponds with length of beams, we assume that the total length for flexures is necessarily equal in both comb drives. Then, we have:

$$10\mu m+(4\times a)\times 4+10\mu m=10\mu m+(2\times\pi\times r)\times 4+10\mu m$$
$$\rightarrow a = 0.5 \times \pi \times r$$

Therefore, we choose r = 15 μm as the radius of the circular curve and a = 23.56 μm as the length of one side of the square in serpentine flexures.

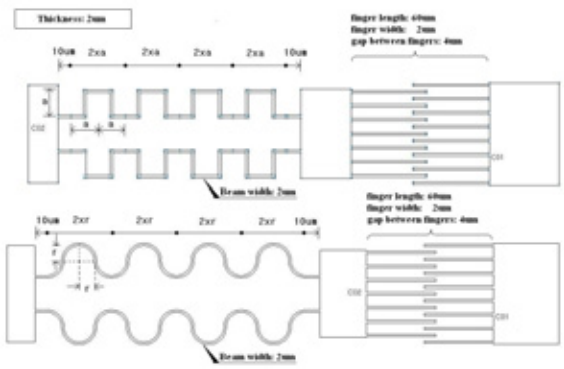

Figure 1. Schematics of the comb drive with rectangular serpentine flexures (upper) and the comb drive with curved serpentine flexures (lower).

2.1 Schematic A

The basic schematic (Schematic A) is described in Figure 2. We choose *Plane Stress (smps)* and *Electrostatics (emes)* in micro electromechanical system (MEMS) mode for COMSOL Multiphysics. In Plane Stress mode, black bold edges on the left and right end edges are given to be fixed, while others are free. In Electrostatic mode, physics of the boundary are *Electric potential* with V_in around the blue area, *Ground* around the gray area, and *Electric continuity* on others. Other detailed subdomain or boundary settings are identical to the comb drive model of MEMS actuator models in COMSOL Model Library [2] Comb drives with RSF have the same settings as those with CSF.

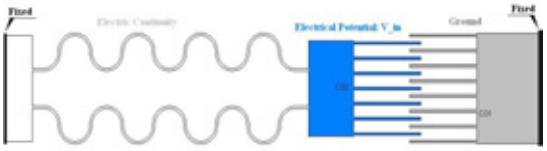

Figure 2. Schematics for comb drives with curved or rectangular serpentine flexures.

2.2 Schematic B

Since Schematic B is for the Q factor, we are going to experiment with resonance in the devices. So, *Solid, Stress-Strain (smsld)* and *Film Damping (mmfd)* are chosen for Multiphysics (go to MEMS Module> Structural Mechanics>Solid, Strain with Film Damping and select *Frequency response analysis*). To simplify simulations, comb parts on the right side in Figure 1 are removed and substituted by applying a driving force (see Figure 3). The lower part in Figure 3 is a view of the model in *xz* plane, and it is selected as Film Damping. Other specific settings are assumed to be identical to the MEMS_gyroscope model in the COMSOL Model Library [3].

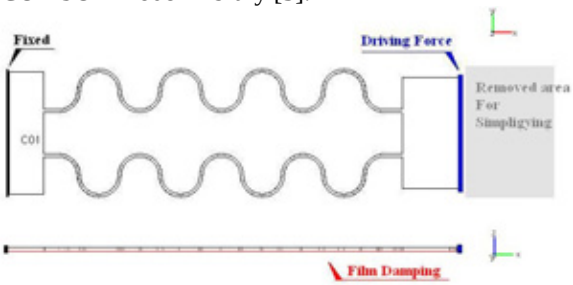

Figure 3. Schematics B and its setting.

2.1 Schematic C

Schematic C is for examining electrical conductivity and thermal conductivity of our devices. Observing only the flexure part in Schematic C is enough to analyze electrical and thermal conductivity. We are therefore going to take only the part between an anchor and a comb in Schematic A (see Figure 4). Its design is based on a model "Joule Heating in a MEMS Device" model [4]. This schematic is drawn on *Heat Transfer by Conduction (ht)* and *Conductive Media DC (dc)* in COMSOL Multiphysics. In Conductive Media DC mode, driving Voltage V_in is applied on one end of the flexure and Ground is on another end. In the Heat Transfer by Conduction setting, the bottom surface is thermal insulation, other surfaces are heat flux. This is because heat outflow on the surface is circumvented by the bottom plane.

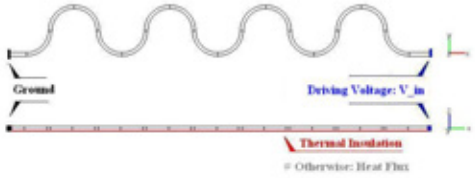

Figure 4. Schematic C and its setting

3. Results and Discussion

3.1 Geometric Process Variations

Voltage [V]	RSF [μm]	CSF [μm]
100	7.55	10.87
200	30.18	43.49
300	67.9	97.86
400	120.7	174
500	188.6	271.8
600	271.6	391.4

Table 1: Results of *x* displacement and its comparison with the RSF and the CSF

Table 1 allows us to compare displacement along the *x*-axis. For all of the given voltage range, *x* displacement in the CSF comb drive is 144% of that of RSF. It is obvious that CSF comb drives have better geometric process variation. Plots of displacement over voltage are given in Figure 5. On the plots, *x* displacement increases as the supplied voltage V_in is raised from 0 V to 600V in CSF and RSF comb drives.

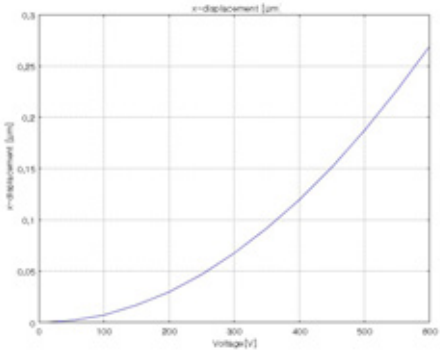

Figure 5-1: Plot of *x* displacement on RSF vs. supplying voltage

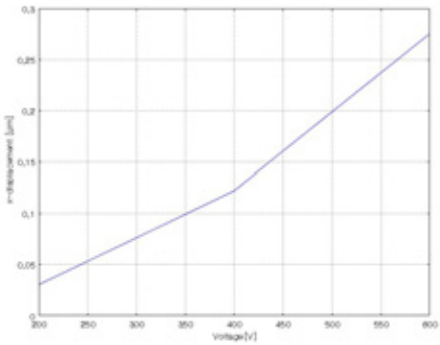

Figure 5-2: Graph of *x* displacement on CSF vs. supplying voltage

Figure 6 shows plots of *y* displacement against voltage. The plot of the RSF has a smoothly increasing curve (Figure 6-1), while the CSF has zero displacement (Figure 6-2). Their displacements are less than 1.3 nm even when the supplying voltage is 600 V and are small enough to suppose that *y* displacement is 0nm.

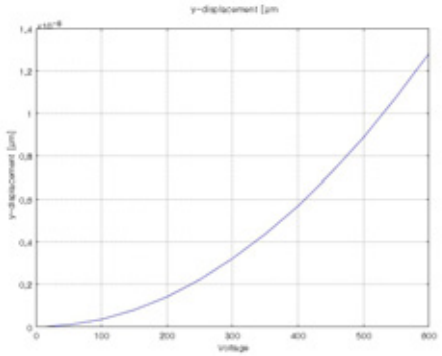

Figure 6-1: Plot of y displacement on RSF vs. supplying voltage

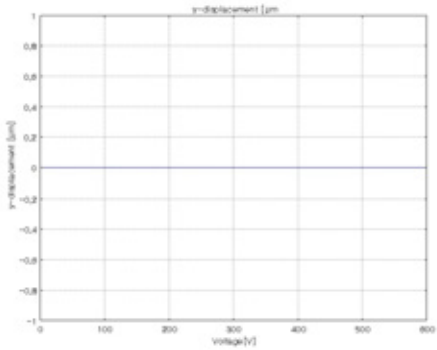

Figure 6-2: the plot of y displacement on CSF vs. supplying voltage

3.2 Linear Range

It is a noticeable fact from the above plots that CSF comb drives have significantly improved linear characteristics. While the RSF has an increasingly curved shape (Figure 5-1), the CSF has linearity (Figure 5-2). Slope is equal to the instant speed (m/V) of *x* displacement according to supplying voltage. The slope of the CSF increases rapidly when supplying voltage is larger than 400 V. In spite of the slope change at 400 V, the linearity range is broad enough to suggest superiority of CSF comb drives for a linear actuator.

Therefore, we conclude that the CSF comb drive shows better performance in an aspect of geometric process variations and linearity range.

3.3 Stress

Plots of Von Mises Stress on the surfaces of two comb drives when the supplying voltage is 600 V (are shown in Figures 7 and 8). Both types of comb drives display higher stress in the serpentine flexure rather than in other parts such as anchor and comb fingers. The RSF is highly stressed on each conjunction of the two flexure edges, and is expected to damage the edge in the long run (see Figure 7)

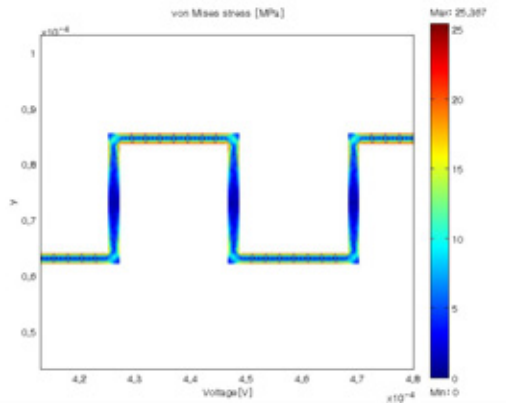

Figure 7. Von Mises Stress on the RSF

While the CSF also is stressed on boundaries of flexures, mid of flexures are significantly low-stressed and connected continuously compare to the RSF (see Figure 8). It will not be injured as much as the RSF.

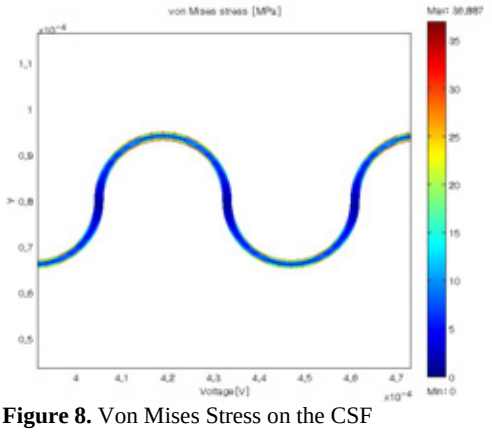

Figure 8. Von Mises Stress on the CSF

The maximum of Von Mises Stress is 25.37 MPa for the RSF and 36.887 MPa for the CSF. Flexures of the CSF are pressured by stress higher than that of the RSF. However, the Von Mises Stress is inappropriate for analysis stress data because this is a RMS (root mean square) value, which combines directional components. We therefore need to check shear stress in the *x* or *y* direction (Tables 2 and 4).

Because stress is directly proportional to the displacement increment, it is reasonable that the shear stress in the *x*-direction increases if *x* displacement increases. *x* Displacement increases 144% (see Table 1), while the *x*-directional shear stress increases 127% (see Table 2) by replacing RSF with CSF. This result explains the superior structure of CSF that the stress rooted by increment of *x* displacement is attenuated in the CSF. For this reason, the change in *x* directional shear stress is less than the change in *x* displacement when RSF is replaced by CSF (see Table 4).

Voltage [V]	RSF [MPa]	CSF [MPa]
100	0.730	0.927
200	2.920	3.709
300	6.569	8.346
400	11.678	14.838
500	18.247	23.184
600	26.276	33.385

Table 2. *x* Directional shear stress and its comparison with the RSF and the CSF

Voltage [V]	RSF [MPa/μm]	CSF [MPa/μm]
100	96.69	85.28
200	96.75	85.28
300	96.75	85.29
400	96.75	85.28
500	96.74	85.30
600	96.74	85.30

Table 3. Ratio of stress against *x* displacement and its comparison with the RSF and the CSF

In addition, we confirm directional shear stress improvement on the CSF (see Table 4). At each supplying voltage, the RSF suffers higher *y* directional shear stress, which means that the RSF has to endure more *y* directional stress than the CSF does (directional stress of the CSF is 59.9% of the RSF). This is another advantage of the CFS structure, in addition to the *x* directional stress attenuation.

Voltage [V]	RSF [MPa]	CSF [MPa]
100	0.607	0.346
200	2.427	1.454
300	5.460	3.272
400	9.707	5.816
500	15.167	9.088
600	21.841	13.087

Table 4. *y* Directional shear stress and its comparison with the RSF and the CSF

We therefore have evidence that the CSF is better for stress management than the RSF in comb drives.

3.4 Strength of Electrical Field

As shown in Figure 2, the left comb has an electric potential V_in and the right comb has Ground. So, an electric field is induced in a space between the two combs, and the comb drives behave like a capacitance. Figure 9 shows the electric field around the fingers when the supplying voltage is 600 V. Maximum values are 263 V/μm in the RSF and 265.5 V/μm in the CSF. The CSF generates a stronger electric field than the RSF does.

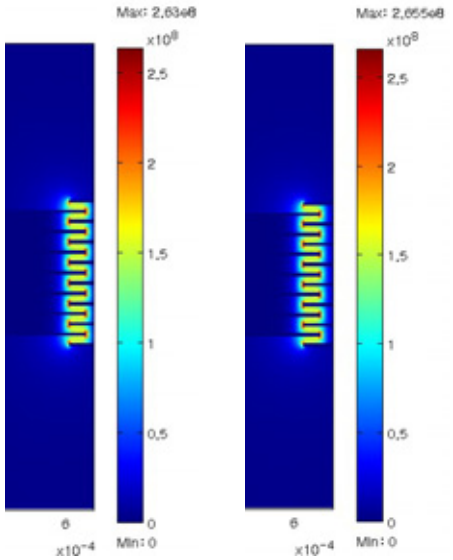

Figure 9-1(left): Plot of the electric field in the RSF
Figure 9-2(right): Plot of the electric field in the CSF

The maximum values of electric field distribution shown in the plot are presented and compared in Table 5. The magnitude of the electrical field around the CSF is larger than the RSF at other voltages. The electric field in the CSF is 100.9% of that of the RSF.

Voltage [V]	RSF [V/μm]	CSF [V/μm]
100	43.84	44.25
200	87.68	88.5
300	131.5	132.7
400	175.4	177
500	219.2	221.2
600	263	265.5

Table 5. Maximum magnitude of the electric field and its comparison with the RSF and with the CSF

3.5 Quality Factor

To compute the Q factor, the resonant frequency is estimated from eigen-frequency (*f*) analysis. Then parametric analysis of eigenvalues suggests lambda (λ) values. Among the derived eigenvalues, we choose an eigenvalue whose imaginary part equals $2\pi \times f$ rad/sec (see Table 6). In these cases, the imaginary part of the first eigenvalue is equal to the λ value we are looking for.

	RSF	CSF
f [Hz]	10146.57	7782.89
$2\pi \times f$ [rad/sec]	63716	48870.96
eigenvalues from parametric analysis	-0.0578 ± 63752.76i -905.44 ± 131646.1i -1.6149 ± 377706.5i	-0.0353 ± 48901.32i -905.43 ± 99809.61i -1.5443 ± 345295.3i
λ	-0.0578 ± 63752.76i	-0.0353 ± 48901.32i

Table 6. Analysis for calculation of resonant frequency

After λ computation, the Q factor is evaluated by an equation: $Q = 0.5 \times \text{abs}(\text{Im}(\lambda)/\text{Re}(\lambda))$. The Q factor of the RSF is 551758 Hz = 0.55 MHz and that of the CSF is 692735.7 Hz = 0.69 MHz.

So, the Q factor of the CSF is 125% of the Q factor of the RSF, and thus we demonstrate that there is a significant quality improvement for better in the CSF.

3.6 Electrical Conductivity

Plots of current versus voltage in Figure 10 are for identifying electrical conductivity as supplying voltage moves from 0 V to 600 V. Straight lines passing through the zero point

appear on the plots. The slope of the lines indicates electrical conductivity. Electrical conductivity in the RSF is 0.2963 A/V and that in the CSF is 0.3123 A/V, which is 105% the electrical conductivity of the RSF. Hence, it is obvious that the CSF contains higher electrical conductivity compared to the RSF.

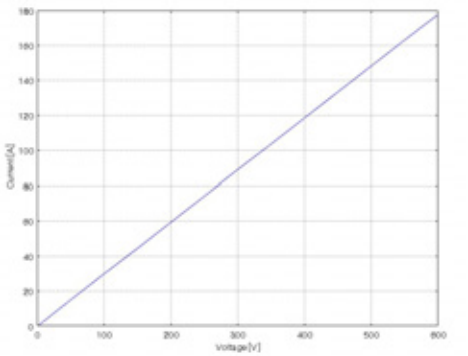

Figure 10-1. Plot of current against voltage in the RSF; its slope shows electrical conductivity

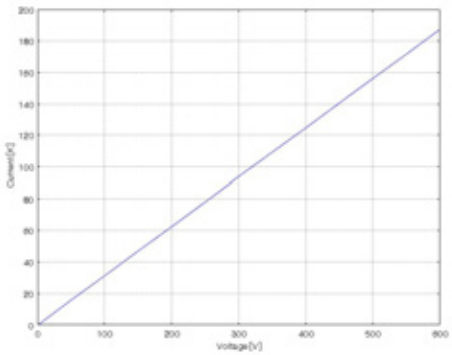

Figure 10-2. Plot of current against voltage in the CSF; its slope shows electrical conductivity

3.7 Thermal Conductivity

To probe thermal conductivity, we plot heat flux (W/m^2) versus temperature gradient (K/m) when supplying voltage changes from 0 V to 600 V (see Figure 11). The slopes of the lines in the plots are the same as thermal conductivity. Thermal conductivity of the RSF is 204.51 W/m· K and thermal conductivity of the CSF is 204.50 W/m·K. These values appear to be close enough to conclude that these two thermal conductivity values are the same. Consequently, thermal conductivity is identical for the RSF and the CSF.

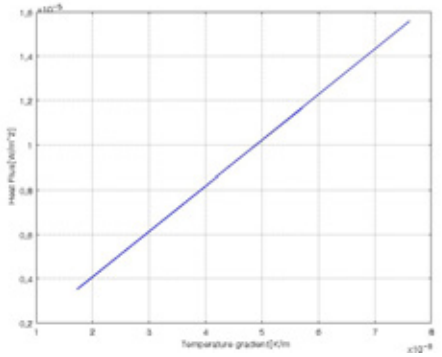

Figure 11-1. The plot of Heat flux against Temperature gradient in the RSF, and its slope is thermal conductivity

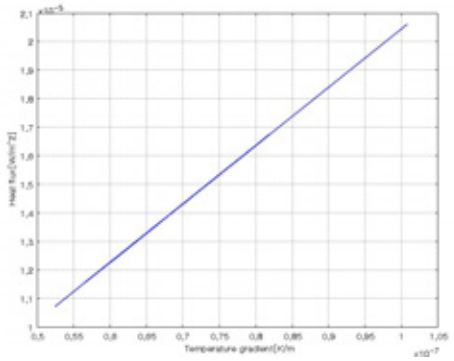

Figure 11-2. The plot of Heat flux against Temperature gradient in the RSF, and its slope is thermal conductivity

4. Conclusions

We have compared the RSF comb-drives and the CSF comb drives with respect to geometric process variations, linear range, stress, strength, quality factor, electrical conductivity, and thermal conductivity. When the supplying voltage is varied, the *x* directional displacement also increases proportionally with the voltage. The ratio of the *x* displacement of the CSF with that of the RSF is 144%, showing that the CSF has broader geometric process variations. The *y* directional displacement of the CSF appears to be almost zero. In the plot of the *x* displacement versus the supplying voltage, we observe that the RSF has a smoothly increasing curve and the CSF has a straight line. This suggests that linearity is significantly improved in CSF comb drives. Since stress is proportional to displacement, theoretically, the ratio of the *x*

directional shear stress of the CSF to that of the RSF is around 144%. But the ratio of that in our simulation is given 127%. Stress handling of the arch structure in the CSF accounts for the results. In addition, the *y* directional stress of the CSF decreased to 59.9% of that of the RSF, which proves that the structure of the CSF is appropriate for stress endurance. The electric field in the CSF is also more intensively distributed. The Q factor in the CSF is considerably higher, 125% that of RSF. Also, the electrical conductivity increases in the CSF, while there is no major difference in thermal conductivity between the CSF and the RSF. Therefore, based on the results from our study, we recommend that CSF comb drives replace RSF comb drives. Certainly, further studies on the characteristics of CSF are needed.

5. References

1. QinShi, et. al., Design Principle of Suspension of MEMS Gyroscope, Southeast University, China (2009)
2. MEMS Actuator Models – MODEL Module Model Library, COMSOL User Document, pp. 7- 145, COMSOL AB (2007)
3. Estimating the Q Factor of a MEMS Gyroscope – MODEL Module Model Library, COMSOL AB (2008)
4. Acar, Robust Micromachined Vibratory Gyroscopes, Ph.D. thesis, Univ. of California, Irvine (2004)
5. Joule Heating in a MEMS Device – MODEL Module Model Library, COMSOL AB (2008)